Lithuanian Journal of Physics, Vol. **61**, No. 2, pp. 84–90 (2021)

ORIGIN OF THERMAL QUENCHING OF EXCITON PHOTOLUMINESCENCE IN AlGaN EPILAYERS

O. Kravcov, J. Mickevičius, and G. Tamulaitis

Institute of Photonics and Nanotechnology, Vilnius University, Saulėtekio 3, 10257 Vilnius, Lithuania
Email: kravcovas@gmail.com; juras.mickevicius@ff.vu.lt

Received 11 May 2021; accepted 13 May 2021

Dynamics of a low-density exciton system is simulated using the kinetic Monte Carlo algorithm. The temperature dependences of photoluminescence (PL) intensity and PL band Stokes shift in a high-Al-content AlGaN epilayer are calculated and fitted to the experimentally measured ones. The key features of nonradiative recombination via delocalized states and direct tunnelling to nonradiative recombination centres and their influence on PL efficiency are analysed. A strong influence of the tunnelling-based recombination in AlGaN epilayers with a large ratio between the densities of nonradiative recombination centres and localized states is revealed.

Keywords: III-nitrides, carrier localization, Monte Carlo simulations, exciton hopping, nonradiative recombination

PACS: 78.55.-m, 78.20.Bh, 73.50.Gr

1. Introduction

Quantum efficiency of photoluminescence (PL) in semiconductor materials and their heterostructures decreases with increasing temperature. Regardless of the specific quenching mechanism, the temperature dependence of the spectrally-integrated PL intensity is usually described by the expression

$$I(T) = \frac{I_0}{1 + \sum_i c_i \exp\left(-\frac{E_{Ai}}{k_B T}\right)}, \quad (1)$$

where I_0 is the low-temperature PL intensity, c_i and E_{Ai} are the rate constant and activation energy of the ith process, and i is the number of nonradiative recombination channels, typically ranging from 1 to 3 [1–9]. The thermally-activated mechanisms responsible for the PL quenching are usually related to the thermal dissociation of free or bound excitons [1–3], escape of carriers out of a quantum well [3, 4], transfer of carriers over a barrier to nonradiative recombination centres [5, 6], and thermal activation of localized carriers [4, 6–9].

The mechanism of carrier delocalization is commonly used to interpret the PL temperature dynamics in materials having a large density of localized states, e.g. ternary nitride alloys, InGaN [6, 7] and AlGaN [8, 9]. However, a few distinct activation energies are hardly compatible with a wide and continuous energy distribution of localized states. An alternative approach is based on the concepts of carrier transport in disordered semiconductors [10, 11]. Such approach takes into account not only the interplay between radiative and nonradiative processes, but also the dynamic exchange of carriers between localized states. The temperature dependence of PL intensity in disordered semiconductors has been shown to be determined both by carrier localization energy scale and the relative concentration of nonradiative centres [11, 12]. However, while the main mechanism of nonradiative recombination is linked to the carrier delocalization, an alternative channel of direct tunnelling to nonradiative centres is usually neglected [13].

In the current paper, we combined both approaches to analyse the thermal quenching of PL intensity in AlGaN epilayers. Exploiting Monte

Carlo simulations to reproduce the PL characteristics and their dependence on temperature, and introducing different recombination mechanisms step-by-step into the model enabled us to reveal the influence and importance of these mechanisms for exciton dynamics and PL properties in the temperature range from 8 to 300 K. We show that the mechanism of exciton tunnelling to nonradiative centres cannot be neglected at high relative densities of nonradiative centres. Moreover, this mechanism has a strong impact on PL intensity already at the lowest temperatures.

2. Experiment

A single AlGaN epilayer distinguished by strong carrier localization was selected for the study. The $Al_{0.65}Ga_{0.35}N$ epilayer was grown by migration-enhanced metalorganic chemical vapour deposition (MEMOCVD®) on the c-plane sapphire substrate. The photoluminescence was measured under quasi-steady-state excitation conditions. The 5th harmonic (213 nm) of the Q-switched YAG:Nd laser radiation (pulse duration 4 ns) was used for excitation. A closed-cycle helium cryostat enabled the variation of temperature in the range from 8 to 300 K. The PL signal was analysed by a double monochromator (*Jobin Yvon* HRD-1) and detected by a UV-enhanced photomultiplier.

3. Theoretical model and Monte Carlo simulation procedures

The model of carrier dynamics that we use for our simulations of PL properties is based on the modified exciton hopping model [11, 14, 15]. In this model, electrons and holes generated by optical excitation rapidly form strongly correlated pairs of excitons, which behave like single non-interacting particles that can be trapped by localizing potential. Localized excitons can recombine radiatively, hop to another localized state or to the mobility edge and become delocalized, or tunnel to a nonradiative recombination centre (NRC). Delocalized (free) excitons can be captured by either a localized state or a NRC. The radiative recombination of free excitons is assumed much slower than the capture processes and is, therefore, neglected. All the kinetic processes considered in the model are schematically illustrated in Fig. 1(a). The rates (probabilities) of different processes are described by formulae presented below.

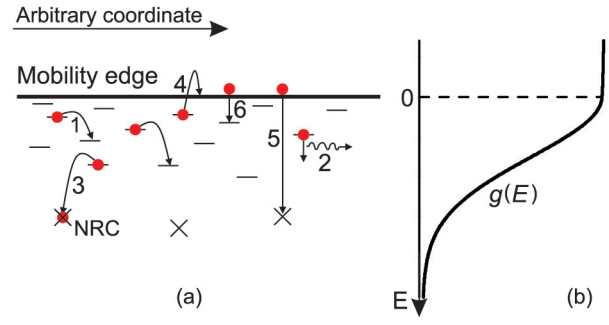

Fig. 1. (a) A schematic illustration of the processes involved in the model of exciton dynamics: hopping transitions between localized states (1), radiative recombination (2), tunnelling to NRC (3), delocalization to the mobility edge (4), capture to NRC (5) and capture to localized state (6). (b) Schematic energy distribution of localized states in the band tail. The origin of energy axes is set to the mobility edge.

The localized excitons can move through the localized states at the rate of hopping from site i to site j calculated using the well-known Miller–Abrahams formula

$$\nu_{i\to j} = \nu_0 \exp\left(-\frac{2R_{ij}}{\alpha}\right)\exp\left(-\frac{E_j - E_i + |E_j - E_i|}{2k_B T}\right), \quad (2)$$

where E_i and E_j are the energies of the initial and final states, respectively, R_{ij} is the distance between the states in real space, α is the decay length of exciton wavefunction, and ν_0 is the attempt-to-escape frequency.

The radiative recombination rate equals the inverse of exciton lifetime,

$$\nu_{\text{rad}} = \tau_0^{-1}. \quad (3)$$

The rate of nonradiative recombination of localized excitons is determined by the probability of tunnelling to NRCs, that depends on the spatial distributions of both NRCs and localized states. Using Eq. (2) and assuming that deep levels act as NRCs, the rate of exciton tunnelling to NRC is described as

$$\nu_{\text{tunnel}} = \nu_0 \exp\left(-\frac{2R_{i,\text{NRC}}}{\alpha}\right), \quad (4)$$

where $R_{i,\text{NRC}}$ is the distance from the localized state to NRC.

The carrier delocalization is considered as a vertical transition in energy space to the mobility edge at the rate

$$\nu_{\text{deloc}} = \nu_0 \exp\left(-\frac{\Delta E}{k_B T}\right), \tag{5}$$

determined by $\Delta E = E_{\text{me}} - E_i$, the energy difference between the mobility edge E_{me} and localized state E_i.

A free exciton can be captured to any localized state at the rate

$$\nu_{\text{capr}} = \nu_0 \frac{N_{\text{loc}}}{N}, \tag{6}$$

whereas the rate for the capture of free excitons by NRCs is described by a similar expression

$$\nu_{\text{capnr}} = \nu_0 \frac{N_{\text{NRC}}}{N}. \tag{7}$$

Here $N = N_{\text{loc}} + N_{\text{NRC}}$ is the total density of localized states and NRCs.

The simulations have been performed using the kinetic Monte Carlo algorithm. The simulation procedure starts by creating a 4D space-energy grid with three spatial and one energy dimensions. The localized states and nonradiative recombination centres with densities N_{loc} and N_{NRC}, respectively, are randomly generated within the grid. The energy distribution of the localized states $g(E)$ is assumed to be Gaussian

$$g(E) = \frac{N_{\text{loc}}}{\sqrt{2\pi\sigma^2}} \exp\left(-\frac{(E - E_{\text{me}})^2}{2\sigma^2}\right), \tag{8}$$

with the energy scale defined as the standard deviation for the potential fluctuations σ [16, 17]. No correlation between the energies of the localized states and their spatial positions is allowed.

Next, a single exciton is generated randomly within the grid. The rates of all possible transitions are calculated using Eqs. (2–7), as described above, and the process is selected randomly. This procedure is repeated until the exciton recombines. For a given distribution of localized states and NRCs, the simulations are repeated many times in order to obtain reliable results. The PL spectrum is accumulated by summing the contribution of each radiative recombination event. Since experimentally obtained PL spectra are typically collected from the area much larger than the simulation grid, the simulations are repeated for a large number of different random distributions of localized states.

4. Results and discussion

The simulations of exciton dynamics and, consequently, of PL properties has been performed by stepwise introduction of different processes into the model describing exciton dynamics. This approach enabled us to reveal the importance of the processes, study the influence of the parameters defining the rate of the processes and link the parameters with the material properties.

At low excitations, the radiative recombination of localized excitons is the dominant radiative process. The PL band shape is generally determined by the distribution function of localized states and parameters $\nu_0\tau_0$ and $N\alpha^3$, which govern the localized exciton hopping process in time and space, respectively [14, 15]. Meanwhile, the PL intensity (and efficiency) is governed by the ratio $N_{\text{NRC}}/N_{\text{loc}}$, which controls the influence of nonradiative recombination [11, 15].

To evaluate the energy scale of the distribution of localized states as well as estimate the values of exciton hopping parameters $\nu_0\tau_0$ and $N\alpha^3$, we exploited the temperature dependence of the Stokes shift (defined as the difference between the PL band peak position and the mobility edge) shown in Fig. 2. The measured PL Stokes shift slightly

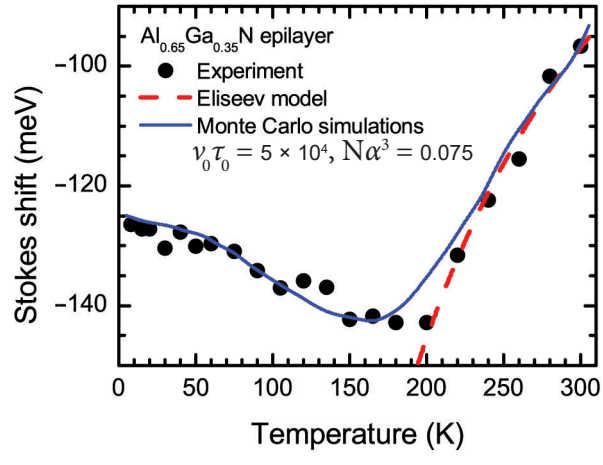

Fig. 2. The temperature dependence of Stokes shift in the AlGaN epilayer with Al content of 65%. Lines show the fits using the Eliseev model (dashed line, red online) and Monte Carlo simulations (solid line, blue online).

increases with increasing temperature approximately in the range from 8 to 200 K and decreases at elevated temperatures up to 300 K. A simple quantitative model of band tail filling, also referred to as Eliseev model [16], reproduces the Stokes shift decrease at elevated temperatures, as indicated by a red (online) dashed line in Fig. 2. The application of the Eliseev model in this temperature range enables estimation of the dispersion parameter describing the energy distribution of localized states (σ = 50 meV for the $Al_{0.65}Ga_{0.35}N$ epilayer presented in Fig. 2). Meanwhile, the increase of the Stokes shift as well as its low-temperature value was successfully simulated using the exciton hopping model, and allowed estimating the hopping parameters $\nu_0\tau_0 = 5 \times 10^4$ and $N\alpha^3 = 0.075$. The simulated Stokes shift dependence is presented by a blue (online) solid line in Fig. 2, and a good agreement with the experimental points is achieved.

The determination of simulation parameters that influence the radiative recombination enabled us to simulate the temperature dependence of PL intensity, which is strongly affected by the nonradiative recombination. The temperature dependence of PL intensity measured under quasi-steady-state excitation is presented in Fig. 3. In the selected high-Al-content epilayer, the PL intensity decreases, albeit slowly, already at low temperatures. The decrease becomes substantially faster at elevated temperatures. The experimental points might be well fitted using Eq. (1) with $i = 2$ (a dashed line, red online, in Fig. 3) implying involvement of two nonradiative channels with activation energies of 6 and 69 meV. These channels might be tentatively attributed to the exciton redistribution within the localized states and exciton delocalization to the mobility edge, respectively [9].

To link the activation energies to the specific exciton transfer and/or recombination processes, we simulated the exciton dynamics by considering two nonradiative recombination mechanisms: i) exciton delocalization to the mobility edge followed by its capture by a NRC and ii) direct tunnelling to a NRC. To reveal the importance of each mechanism, we first analyse their impact on the temperature dependence of PL intensity separately.

The exciton delocalization and subsequent capture by NRCs is considered to be the main mechanism of nonradiative recombination in the exciton hopping models presented in literature [11–13, 15]. This mechanism is governed by the relative density of nonradiative and localized centres N_{NRC}/N_{loc} and by the temperature. The curves of PL efficiency as a function of temperature simulated for several values of parameter N_{NRC}/N_{loc} are presented in Fig. 4(a). At low temperatures, the efficiency is practically unaffected and remains close to 100%.

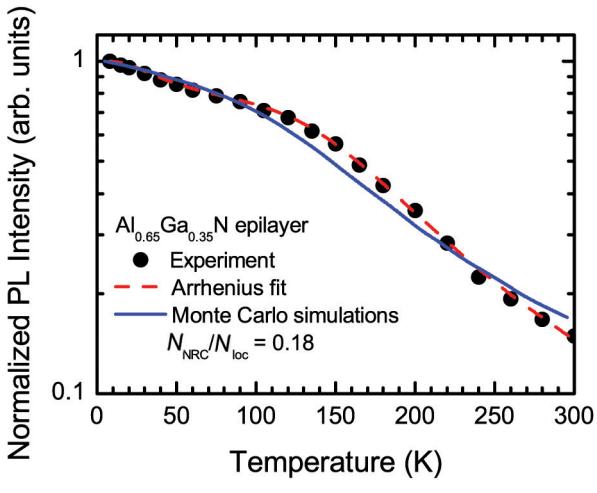

Fig. 3. The temperature dependence of integrated PL intensity in the AlGaN epilayer with Al content of 65%. Lines show the fits using Eq. (1) (dashed line, red online) and Monte Carlo simulations (solid line, blue online).

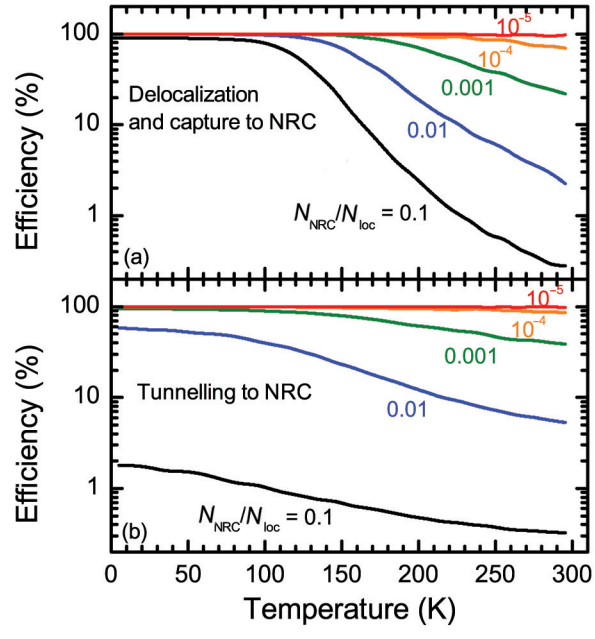

Fig. 4. The simulated PL efficiency dependences on temperature for different nonradiative recombination mechanisms: delocalization and capture to NRCs (a) and direct tunnelling to NRCs (b).

The temperature for the onset of efficiency decrease and the decrease rate afterwards depend on the ratio N_{NRC}/N_{loc}. As the ratio increases, the PL efficiency decrease onset shifts to lower temperatures, which, in turn, results in a lower room-temperature efficiency. This mechanism is basically a two-step process, thus, the low probability of delocalization ensures almost temperature-unaffected PL intensity at low temperatures. The PL intensity dependences on temperature for this mechanism can be described by Arrhenius-type Eq. (1) with a single thermally-activated channel with activation energy E_A in the range from 107 to 120 meV, and the rate constant c, which reflects the strength of this mechanism and correlates with the parameter N_{NRC}/N_{loc}.

The rate of direct exciton tunnelling to NRCs depends on how many NRCs are in the close vicinity of a given localized state, thus, this mechanism is governed only by the density of nonradiative centres relative to the density of localized states, described by the parameter N_{NRC}/N_{loc}. The simulated PL efficiency curves are shown in Fig. 4(b) for several values of this parameter. Usually, the ratio N_{NRC}/N_{loc} is assumed to be small and the process of exciton tunnelling to NRC is neglected [13]. Indeed, for low densities of NRCs, only a slight decrease of the PL efficiency is observed at high temperature, as shown in Fig. 4(b). However, the increase in the ratio N_{NRC}/N_{loc} results in a significant decrease of the low-temperature efficiency value and a gradual decrease starting already at low temperatures. The former feature is consistent with the previously reported experimental results [12, 18], whereas it is not observed for the nonradiative recombination via delocalized states (see Fig. 4(a)) discussed above. The Arrhenius-type description of PL intensity dependences for the tunnelling mechanism requires two thermally-activated channels with activation energies of the order of 7 and 50 meV.

Comparing the experimental PL intensity dependence (see Fig. 3) with the simulated curves of Fig. 4, several features might be pointed out. A quite significant decrease of PL intensity within the temperature range between 8 and 100 K, observed in the experimentally obtained dependence, implies a strong influence of the direct tunnelling mechanism. Moreover, a high ratio of the measured PL intensities at room and low temperatures, $I_{PL,\,300K}/I_{PL,\,8K} = 0.15$, indicates a large value of the parameter N_{NRC}/N_{loc}. Thus, the tunnelling mechanism cannot be neglected, and the simulations of PL intensity must include both nonradiative recombination mechanisms. The simulated curve is shown by a blue (online) solid line in Fig. 3. An adequate agreement has been achieved using the N_{NRC}/N_{loc} value of 0.18.

Thus, the fitting of simulated and measured dependences revealed that the temperature dependence of PL intensity could not be properly described by taking into account the nonradiative recombination only via delocalized states. The tunnelling to NRCs causes a significant decrease in the low-temperature efficiency value and a gradual decrease in the temperature range where the first mechanism is insignificant. The lower activation energy extracted from the fit using Eq. (1) serves as an indicator of the strong tunnelling mechanism. At temperatures elevated above 100 K, the efficiency decrease might be described by the Arrhenius-type functions for both nonradiative recombination mechanisms. Therefore, the higher activation energy extracted from the fit using Eq. (1) represents an effective average of both processes, except for the epilayers with the low ratio N_{NRC}/N_{loc} when the nonradiative recombination proceeds predominantly via delocalized states.

5. Conclusions

To summarize, we simulated the dynamics of a low-density exciton system using the kinetic Monte Carlo algorithm and calculated the temperature dependence of PL intensity in a high-Al-content AlGaN epilayer to fit it to the experimentally measured dependence. The temperature dependence of the Stokes shift between the mobility edge and the peak position of PL band has been exploited to estimate the parameters necessary for the simulations. The study included two nonradiative recombination mechanisms: recombination via delocalized states and direct tunnelling to NRCs. The analysis and subsequent fitting with experimental results revealed the importance of the direct tunnelling to NRCs in epilayers with a high ratio between the densities of nonradiative recombination centres and localized states, which might be expected in certain III-nitride epilayers, especially in high-Al-content epilayers. The tunnelling to NRCs results in a substantial decrease in the absolute values of low-temperature efficiency

and a gradual efficiency decrease with temperature in the range from 8 to ~100 K. The temperature dependence of the efficiency affected exclusively by nonradiative recombination via delocalized states is negligible in this range for any reasonable material parameters. Thus, the gradual efficiency decrease, that has been observed in the epilayer used for fitting in this paper and in many other III-nitride epilayers, has to be attributed to the influence of direct tunnelling to NRCs. Above ~100 K temperature, both mechanisms cause the efficiency decrease with temperature, that can be described by an Arrhenius-type function. However, except for the cases when the tunnelling effect might be neglected (at low densities of NRCs), the activation energy extracted from such description of experimental dependence is just an empirical parameter that depends on the activation energies for both processes.

The sample of the $Al_{0.65}Ga_{0.35}N$ epilayer, which has been used for fitting the calculated and measured characteristics in this paper, shows that the contribution of exciton recombination via tunnelling to nonradiative recombination centres might be not only important but also dominant over the nonradiative recombination via delocalized states. The features peculiar to the strong influence of tunnelling are observed in many AlGaN epilayers, presumably in those with high densities of NRCs. The conclusion on the importance of tunnelling is also consistent with a low luminescence efficiency at low temperatures, which has been observed experimentally. It supports the instruction to cautiously apply the assumption that the low-temperature efficiency is 100% in estimating the absolute values of photoluminescence efficiency at elevated temperatures.

Acknowledgements

The research was supported by the European Social Fund under Grant Agreement with the Research Council of Lithuania (LMTLT) (Project No. LMT-K-712-01-0076). Support for mobility by COST Action CA17126 is also acknowledged.

References

[1] D. Bimberg, M. Sondergeld, and E. Grobe, Thermal dissociation of excitons bound to neutral acceptors in high-purity GaAs, Phys. Rev. B **4**, 3451 (1971).

[2] M. Hugues, B. Damilano, J.-Y. Duboz, and J. Massies, Exciton dissociation and hole escape in the thermal photoluminescence quenching of (Ga, In)(N, As) quantum wells, Phys. Rev. B **75**, 115337 (2007).

[3] Y. Yang, P. Ma, X. Wei, D. Yan, Y. Wang, and Y. Zeng, Design strategies for enhancing carrier localization in InGaN-based light-emitting diodes, J. Lumin. **155**, 238 (2014).

[4] H.D. Sun, S. Calvez, M.D. Dawson, J.A. Gupta, G.C. Aers, and G.I. Sproule, Thermal quenching mechanism of photoluminescence in 1.55 μm GaInNAsSb/Ga(N)As quantum-well structures, Appl. Phys. Lett. **89**, 101909 (2006).

[5] K.L. Teo, J.S. Colton, P.Y. Yu, E.R. Weber, M.F. Li, W. Liu, K. Uchida, H. Tokunaga, N. Akutsu, and K. Matsumoto, An analysis of temperature dependent photoluminescence line shapes in InGaN, Appl. Phys. Lett. **73**, 1697 (1998).

[6] X.H. Zheng, H. Chen, Z.B. Yan, D.S. Li, H.B. Yu, Q. Huang, and J.M. Zhou, Influence of the deposition time of barrier layers on optical and structural properties of high-efficiency green-light-emitting InGaN/GaN multiple quantum wells, J. Appl. Phys. **96**, 1899 (2004).

[7] M.A. Sousa, T.C. Esteves, N.B. Sedrine, J. Rodrigues, M.B. Laurenco, A. Redondo-Cubero, E. Alves, K.P. O'Donnell, M. Bockowski, C. Wetzel, M.R. Correia, K. Lorenz, and T. Monteiro, Luminescence studies on green emitting InGaN/GaN MQWs implanted with nitrogen, Sci. Rep. **5**, 9703 (2015).

[8] A. Yasan, R. McClintock, K. Mayes, D.H. Kim, P. Kung, and M. Razeghi, Photoluminescence study of AlGaN-based 280 nm ultraviolet light-emitting diodes, Appl. Phys. Lett. **83**, 4083 (2003).

[9] J. Mickevičius, G. Tamulaitis, J. Jurkevičius, M.S. Shur, M. Shatalov, J. Yang, and R. Gaska, Efficiency droop and carrier transport in AlGaN epilayers and heterostructures, Phys. Status Solidi B **252**, 961 (2015).

[10] S.D. Baranovskii, Theoretical description of charge transport in disordered organic semiconductors, Phys. Status Solidi B **252**, 961 (2014).

[11] O. Rubel, S.D. Baranovskii, K. Hantke, B. Kunert, W.W. Ruhle, P. Thomas, K. Volz, and W. Stolz, Model of temperature quenching of photoluminescence in disordered semiconductors and comparison to experiment, Phys. Rev. B **73**, 233201 (2006).

[12] M. Baranowski, R. Kudrawiec, J. Misiewicz, H. Turski, and C. Skierbiszewski, Photoluminescence characterization of InGaN/InGaN quantum wells grown by plasma-assisted molecular beam epitaxy: impact of nitrogen and gallium fluxes, Phys. Status Solidi B **252**, 983 (2015).

[13] K. Jandieri, B. Kunert, S. Liebich, M. Zimprich, K. Volz, W. Stolz, F. Gebhard, S.D. Baranovskii, N. Koukourakis, N.C. Gerhardt, and M.R. Hofmann, Nonexponential photoluminescence transients in Ga(NAsP) lattice matched to a (001) silicon substrate, Phys. Rev. B **87**, 035303 (2013).

[14] S.D. Baranovskii, R. Eichmann, and P. Thomas, Temperature-dependent exciton luminescence in quantum wells by computer simulation, Phys. Rev. B **58**, 13081 (1998).

[15] M. Baranowski, M. Latkowska, R. Kudrawiec, and J. Misiewicz, Model of hopping excitons in GaInNAs: simulations of sharp lines in micro-photoluminescence spectra and their dependence on the excitation power and temperature, J. Phys. Condens. Matter **23**, 205804 (2011).

[16] P.G. Eliseev, P. Perlin, J. Lee, and M. Osinski, 'Blue' temperature-induced shift and band-tail emission in InGaN-based light sources, Appl. Phys. Lett. **71**, 569 (1997).

[17] K. Kazlauskas, A. Žukauskas, G. Tamulaitis, J. Mickevičius, M.S. Shur, R.S. Qhalid Fareed, J.P. Zhang, and R. Gaska, Exciton hopping and nonradiative decay in AlGaN epilayers, Appl. Phys. Lett. **87**, 172102 (2005).

[18] J. Mickevičius, G. Tamulaitis, M. Shur, M. Shatalov, J. Tang, and R. Gaska, Internal quantum efficiency in AlGaN with strong carrier localization, Appl. Phys. Lett. **101**, 211902 (2012).

EKSITONINĖS FOTOLIUMINESCENCIJOS AlGaN EPITAKSINIUOSE SLUOKSNIUOSE TEMPERATŪRINIO GESIMO PRIGIMTIS

O. Kravcov, J. Mickevičius, G. Tamulaitis

Vilniaus universiteto Fotonikos ir nanotechnologijų institutas, Vilnius, Lietuva

Santrauka

Mažo tankio eksitonų sistemos dinamika tirta skaitmeninio modeliavimo metodais naudojant kinetinį Monte Karlo algoritmą. Sumodeliuotos fotoliuminescencijos (FL) intensyvumo ir FL juostos Stokso poslinkio temperatūrinės priklausomybės buvo tapatintos su eksperimentiškai išmatuotomis AlGaN epitaksiniame sluoksnyje su dideliu Al kiekiu. Darbe analizuojamos dviejų nespindulinės rekombinacijos mechanizmų – pagavimo per delokalizuotas būsenas ir tiesioginio tuneliavimo į nespindulinius centrus – savybės ir poveikis FL efektyvumui. Atskleista stipri tuneliavimo mechanizmo įtaka AlGaN epitaksiniuose sluoksniuose, pasižyminčiuose dideliu nespindulinių centrų ir lokalizuotų būsenų tankių santykiu.